ELSEVIER

DRUG DISCOVERY TODAY TECHNOLOGIES

Drug Discovery Today: Technologies

Vol. 31, 2019

Protein degradation for drug discovery

Structurally-defined deubiquitinase inhibitors provide opportunities to investigate disease mechanisms

Ingrid E. Wertz[1,2,*], Jeremy M. Murray[3,*]

[1]Department of Discovery Oncology, Genentech, Inc. 1 DNA Way, South San Francisco, 94080, USA
[2]Department of Early Discovery Biochemistry, Genentech, Inc. 1 DNA Way, South San Francisco, 94080, USA
[3]Department of Structural Biology, Genentech, Inc. 1 DNA Way, South San Francisco, 94080, USA

The Ubiquitin/Proteasome System comprises an essential cellular mechanism for regulated protein degradation. Ubiquitination may also promote the assembly of protein complexes that initiate intracellular signaling cascades. Thus, proper regulation of substrate protein ubiquitination is essential for maintaining normal cellular physiology. Deubiquitinases are the class of enzymes responsible for removing ubiquitin modifications from target proteins and have been implicated in regulating human disease. As such, deubiquitinases are now recognized as emerging drug targets. Small molecule deubiquitinase inhibitors have been developed; among those, inhibitors for the deubiquitinases USP7 and USP14 are the best-characterized given that they are structurally validated. In this review we discuss the normal physiological roles of the USP7 and USP14 deubiquitinases as well as the pathological conditions associated with their dysfunction, with a focus on oncology and neurodegenerative diseases. We also review structural biology of USP7 and USP14 enzymes and the characterization of their respective inhibitors, highlighting the various molecular mechanisms by which these deubiquitinases may be functionally inhibited. Finally, we summarize the cellular and *in vivo* studies performed using the structurally-validated USP7 and USP14 inhibitors.

Introduction

The ubiquitin/proteasome system (UPS) is a highly regulated protein modification pathway whereby the covalent attachment of one or more ubiquitin proteins promotes proteolysis, or other non-proteolytic fates, of substrate proteins [1–6]). Three distinct biochemical activities, represented by E1, E2 and E3 enzymes, are required to conjugate the C-terminus of ubiquitin to the target protein Lys or Thr residues or the amino terminus (Fig. 1) [7–10]. Polyubiquitin chains may be linked via one of the seven ubiquitin Lys residues or via the ubiquitin amino terminus. The various chain linkages confer

*Corresponding authors: I.E. Wertz (ingrid@gene.com), J.M. Murray (murray.jeremy@gene.com)

 https://doi.org/10.1016/j.ddtec.2019.02.003

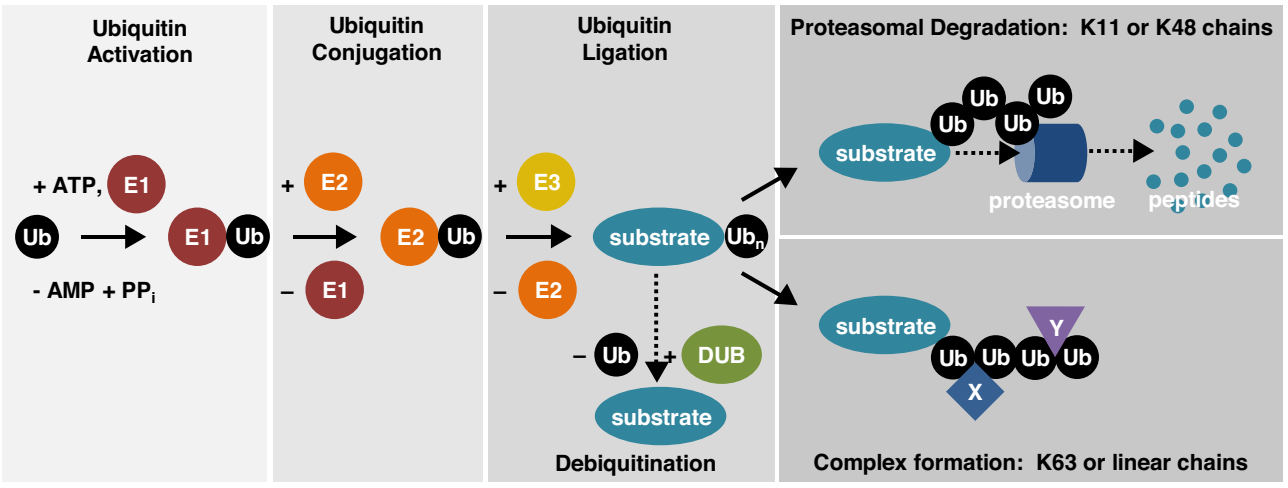

Fig. 1. The ubiquitin/proteasome system. See text for more details. Modified from Ref. [12].

unique chain topologies that in turn dictate different cellular fates of ubiquitin-modified proteins. For example non-degradative polyubiquitin chains, including those comprised of linear or Lys-63 (K63) linkages, promote protein complex formation whereas K11- and K48-linked polyubiquitin chains promote protein degradation [4]. Substrates that are destined for degradation by the proteasome are recognized, unfolded and proteolyzed in a ubiquitin-dependent manner [11]. The regulatory particle (RP) of the proteasome contains a diverse set of ubiquitin receptors that recognize and process the ubiquitinated substrate before proteolysis by the core particle (CP) of the proteasome (Fig. 1) [12]. Deubiquitinating enzymes (DUBs) represent checkpoints in the UPS pathway by removing ubiquitin independent of, or in accordance with, subsequent proteolysis by the proteasome or lysosomal proteases [13]. Improper function of the UPS has been linked to a number of human pathologies including autoimmunity and inflammation, neurodegeneration, and cancer [14]. Targeting protein degradation is now recognized as a promising therapeutic strategy for a number of disease indications [15–18]. Due to recent advances in screening technologies and structural biology, DUBs are increasingly recognized as attractive targets for therapeutic intervention in the treatment of these pathologies [6,19–26].

In humans, DUBs are classified into seven gene families based on sequence and structural similarities: ubiquitin-specific proteases (USPs, 56 members), ovarian tumor proteases (OTU, 14 members), ubiquitin C-terminal hydrolases (UCHs, 4 members), Machado-Joseph disease protein proteases (MJD, 4 members), the motif interacting with ubiquitin (MIU)-containing novel DUB family (MINDY, 4 members), Zinc Finger ubiquitin-specific protease (ZUP/ZUFSP, 1 member), and JAMM/MPN motif proteases (JAMM, 12 members). The USP, OTU, UCH, MJD, MINDY, and ZUP families are all cysteine proteases, containing a catalytic triad of Cys, His and Asp/Asn; in contrast, the JAMMs are zinc-dependent metalloproteases [6,27–33]. Although DUBs represent a diverse group of enzymes, they all contain at least one ubiquitin binding site, the S1 site, that functions to position the conjugated C-terminus of ubiquitin into the catalytic cleft for concomitant hydrolysis.

This common feature of the catalytic mechanism of DUBs forms the basis of DUB activity-based reagents. More specifically, ubiquitin-based fluorogenic substrates are typically comprised of fluorescent dyes, such as Rhodamine-110 or 7-amino-4-methylcoumarin (AMC), conjugated to the C-terminus of ubiquitin [34–36]. Similarly, ubiquitin-based activity probes contain C-terminally conjugated Cys-reactive warheads such as vinyl sulfone or vinyl methyl ester [37]. The fluorogenic substrates enable high-throughput screens of compound libraries to identify small molecule DUB inhibitors, and both activity-based probes and fluorogenic substrates facilitate selectivity profiling of promising leads (for excellent reviews see Refs. [25,26,38,39]). This review will focus on the pathophysiological roles of USP7 and USP14 in oncology and neurology, as well as in-depth structural analysis of potent and specific USP7 and USP14 inhibitors as paradigms for selectively targeting DUBs.

USP7 biology

USP7 in oncology

USP7 (also known as Herpesvirus Associated Ubiquitin-Specific Protease, or HAUSP) is a key regulator of Murine Double Minute-2 (MDM2), a ubiquitin ligase that promotes degradation of the p53 tumor suppressor protein. Interestingly, USP7 has been reported to deubiquitinate and stabilize both p53 and MDM2 [40]. This dual function could result in a futile cycle of p53 ubiquitination and de-ubiquitination. However,

genetic studies indicate that MDM2 is the primary USP7 substrate in unstressed, cycling cells: in USP7-null cells and embryos, p53 accumulates due to MDM2 destabilization [41–43]. Furthermore, USP7 substrate specificity switches upon DNA damage, whereby ATM kinase activation promotes phosphorylation of MDM2 and the related p53 inhibitory protein MDMX. Phospho-MDM2 and -MDMX dissociate from USP7, resulting in their destabilization, subsequent p53 accumulation, and p53-mediated DNA repair or cell death [44]. Thus, USP7 substrates are carefully regulated and context-dependent.

N-Myc, a member of the MYC oncoprotein family, drives neuroblastoma tumorigenesis [45] and is another genetically-validated USP7 substrate. Tavana et al. engineered *Nes-Cre*; *Hausp*$^{fl/fl}$ mice to conditionally express truncated and inactive USP7 in the brain. Upon USP7 functional depletion, N-Myc levels were decreased at the protein, but not the mRNA level [46]. Importantly N-Myc levels were also reduced upon USP7 knockout in the *Trp53*-null background, indicating that USP7 regulates N-Myc independently of the p53 tumor suppressor. Furthermore, USP7 regulation was specific for N-Myc, as c-Myc protein and mRNA levels were unchanged in USP7-deleted cells. The authors also showed that USP7 interacts with N-Myc in cellular and recombinant protein systems, and that USP7 deubiquitinates N-Myc in cells, thus implicating N-Myc as a *bona fide* USP7 substrate. USP7 ablation in N-Myc-amplified neuroblastoma lines attenuated cellular proliferation, and analysis of patient databases revealed that glioblastoma patient samples having elevated USP7 mRNA levels correlated with an N-Myc gene signature and shorter overall patient survival [46].

A number of additional USP7 substrates, that are primarily tumor promoters, have been reported. We refer our readers to recent reports for more comprehensive reviews [47,48]. Here we highlight histone H2B given the association of decreased histone H2B ubiquitination (H2B-Ub) with advanced cancers and the multifaceted evidence supporting regulation of H2B-Ub by USP7 [49]. More specifically, the regulation of H2B-Ub by USP7 in collaboration with the guanosine 5'monophosphate synthetase (GMPS) cofactor is evolutionarily conserved, having first been described in *Drosophila* [50]. Furthermore USP7/GMPS regulation of H2B-Ub is co-opted by the Epstein-Barr virus to enhance transcription from latent origins of replication [51], and structural insights to the allosteric regulation of USP7 by GMPS are reported [52]. Interestingly, sequencing of 633 epigenetic regulatory proteins across 1000 pediatric tumors revealed that inactivating USP7 mutations are associated with pediatric leukemias. Cellular studies confirmed that exogenous expression of the USP7 mutants failed to promote H2B-Ub deubiquitination, however H2B-Ub levels were not evaluated in the tumors [53]. Thus the role of USP7 in regulating oncogenesis via H2B-Ub requires further investigation.

USP7 in neurology

The most definitive data pointing to the essential role of USP7 in regulating neuronal physiology are studies performed on mice in which USP7 is deleted in the brain (*hausp*$\Delta^{Ex6/\Delta Ex6}$) [43]. *Hausp*$\Delta^{Ex6/\Delta Ex6}$ mice are born at expected Mendelian ratios but die shortly after birth due to neurological deficits. The neurodevelopmental deficiencies were primarily, but not exclusively, caused by p53-mediated apoptosis because inactivation of p53 failed to completely rescue the neonatal lethality of the *hausp*$\Delta^{Ex6/\Delta Ex6}$ mice. Thus USP7 is critical for murine brain development due to both p53-dependent and p53-independent roles [43].

USP7 also regulates the TRIM27/MAGE-L2 complex. The Melanoma Antigen-L2 (MAGE-L2) protein is often deleted or mutated in the related Prader–Willi and Schaaf–Yang neurodevelopmental syndromes and also regulates the Tripartite Motif-27 (TRIM-27) ubiquitin ligase. Functional disruption of the TRIM27/MAGE-L2 complex impairs recycling of endosomal proteins to the plasma membrane, leading to their lysosomal degradation [54]. USP7 regulates the stability of the TRIM27/MAGE-L2 complex and thereby modulates protein trafficking through the endocytic pathway [55]. Importantly, USP7 haploinsufficiency results in similar symptoms observed in Prader–Willi and Schaaf–Yang syndrome patients [54]. Whole exome sequencing and chromosome microarray studies have also revealed that patients bearing USP7 mutations present with a related spectrum of neurodevelopmental deficits (for more information, visit https://www.usp7.org/). The collective data suggest that defective membrane protein recycling in the brain due to dysfunction of the TRIM27/MAGE-L2/USP7 complex contributes to neurological and cognitive impairment.

In sum, somatic USP7 inactivation is associated with tumorigenesis, whereas germline USP7 haploinsufficiency is associated with neurodevelopmental disorders. These findings, as well as other mechanisms by which USP7 inhibition attenuates disease [56], have prompted a number of institutions to develop USP7 inhibitors for therapeutic benefit.

Mechanisms of USP7 inhibitors

USP7 structural biology

Ubiquitin-specific protease-7 (USP7) has a modular domain architecture, with an N-terminal TRAF domain (residues 54-208), a catalytic domain (residues 209-560), a series of 5 ubiquitin-like (UBL) domains (residues 561-1083), and a C-terminal regulatory domain (residues 1084–1102). Crystal structures of the isolated domains, structures of domain combinations, and structures of engineered chimeras have provided a wealth of structural insight into the roles of the peripheral domains and how these domains might work together to bind substrate and regulate catalytic activity [57–59,52,60–62].

The crystal structure of USP7 catalytic domain helped to define the structural features of the Ubiquitin Specific Protease (USP) subgroup of DUBs, with the catalytic domain resembling an open hand containing Fingers, Thumb, and Palm subdomains, an architecture that is conserved in all USP domains [57,27,28,29,6] (Fig. 2a). The Fingers subdomain of USP7 is comprised of four β-strands (β1, β2, β4, and β7) and two at the tip of the fingers (β5 and β6). The Thumb subdomain consists of eight α-helices (α1–α6, α9, and α10). The Palm subdomain consists of eight stranded β-sheet (β3, β8–β14), two α-helices (α7 and α8) and several surface loops. A deep cleft around the active site is formed by the packing of six β-strands from the Palm (β8, β10–β14) against the globular Thumb, with the catalytic triad located at the base of the cleft with catalytic Cys223 in the Thumb subdomain and the catalytic His464/Asp481 dyad located in the Palm subdomain.

A number of unexpected details emerged from the crystal structure analysis of the isolated USP7 catalytic domain in its apo-form [57,63]. First is the mis-aligned catalytic triad, with Nδ1 atom of the catalytic histidine (His464) 9.7 Å away from Sγ atom of the catalytic cysteine (Cys223). Second is the conformation of two surface loops, termed blocking loop 1 (BL1; residues 407–429) and blocking loop 2 (BL2; residues 459–462) sterically occluding the catalytic cleft. Third is the loop connecting α4 and α5 helices, termed the switching loop, (residues 284–296) partially occluded access to the catalytic Cys223 (Fig. 2). These three structural details provided insight into why the isolated catalytic domain of USP7 is 120-fold less active than the full-length protein [52,62,64]. The crystal structure of USP7 catalytic domain in complex with ubiquitin aldehyde established the ubiquitin binding site (S1 site), comprised of the Fingers, Palm and α1 and α5 from the Thumb subdomains (Fig. 2c). The C-terminus of ubiquitin sits in the deep cleft between the palm and thumb sub-domains. The covalent interaction between the C-terminal aldehyde and the catalytic Cys223 aligns the catalytic triad and results in the rearrangement of BL1 and BL2 with the Phe409 sidechain moving over 5 Å to accommodate the ubiquitin C-terminus. The switching loop region also undergoes a large conformational change that places the Asp295 sidechain within H-bond distance of the Tyr514 sidechain and the backbone –NH of Val296 makes a H-bond interaction with Tyr465 sidechain [57]. The extent of the differences between the inactive and active conformations of USP7 seem to be unique to USP7 suggesting that USP7 catalytic activity is highly regulated (Fig. 2e & f).

USP7 inhibitor structural biology

Given that all DUBs contain at least one ubiquitin binding site, the S1 site, efficiently developing potent and selective small molecule inhibitors against a particular USP, such as USP7, from a screening hit without a detailed molecular understanding of the binding mode is very challenging. Thus, lack of potency and selectivity were among the problems that plagued the first reported USP7 inhibitors (Fig. 3).

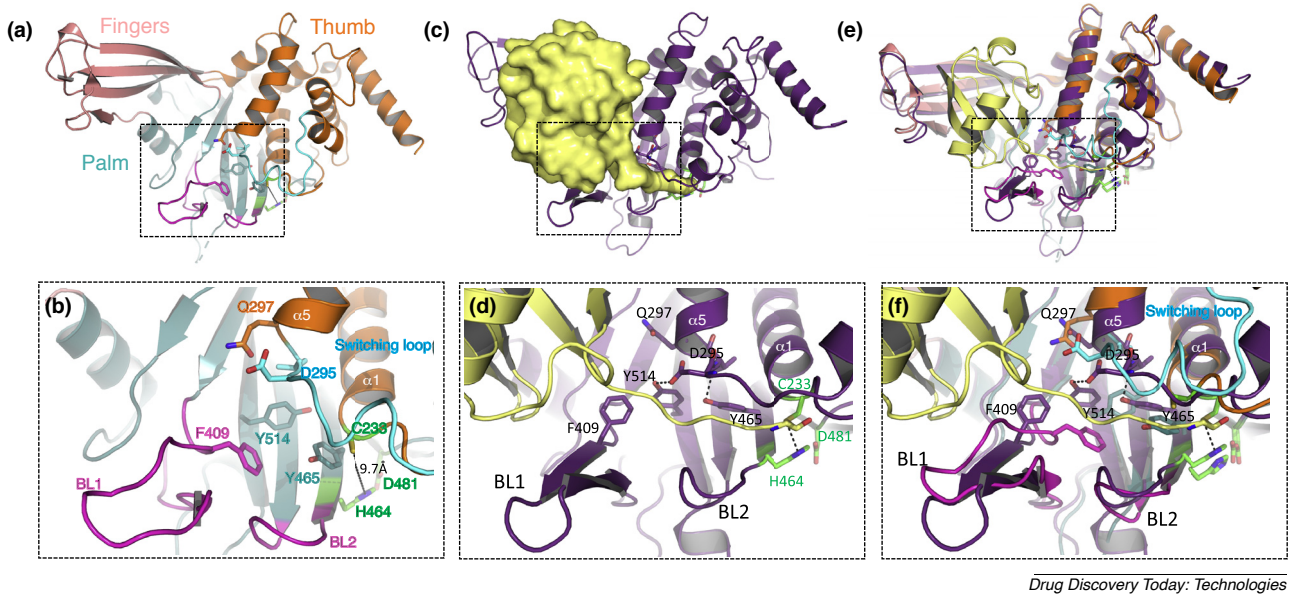

Fig. 2. Crystal structures of USP7 catalytic domain in the inactive (PDB-ID 4M5W) and active conformation with ubiquitin aldehyde (PDB-ID 1NBF). (a) The Fingers, Palm and Thumb sub-domains of inactive USP7 are colored pink, blue and orange respectively. (b) The active site cleft of inactive USP7 with important residues labeled and the catalytic triad colored green. (c) Crystal structure of USP7 catalytic domain in complex with ubiquitin aldehyde. Ubiquitin aldehyde is shown in a surface representation and colored yellow. (d) Active site cleft of USP7 in complex with ubiquitin with important residues labeled and the catalytic triad colored green. (e) Superposition of the inactive and active forms reveals the large conformational changes that occur in α5, the switching loop, BL1, BL2, and the catalytic triad. (f) Comparison of the active site cleft of USP7 in the inactive conformation and in complex with ubiquitin.

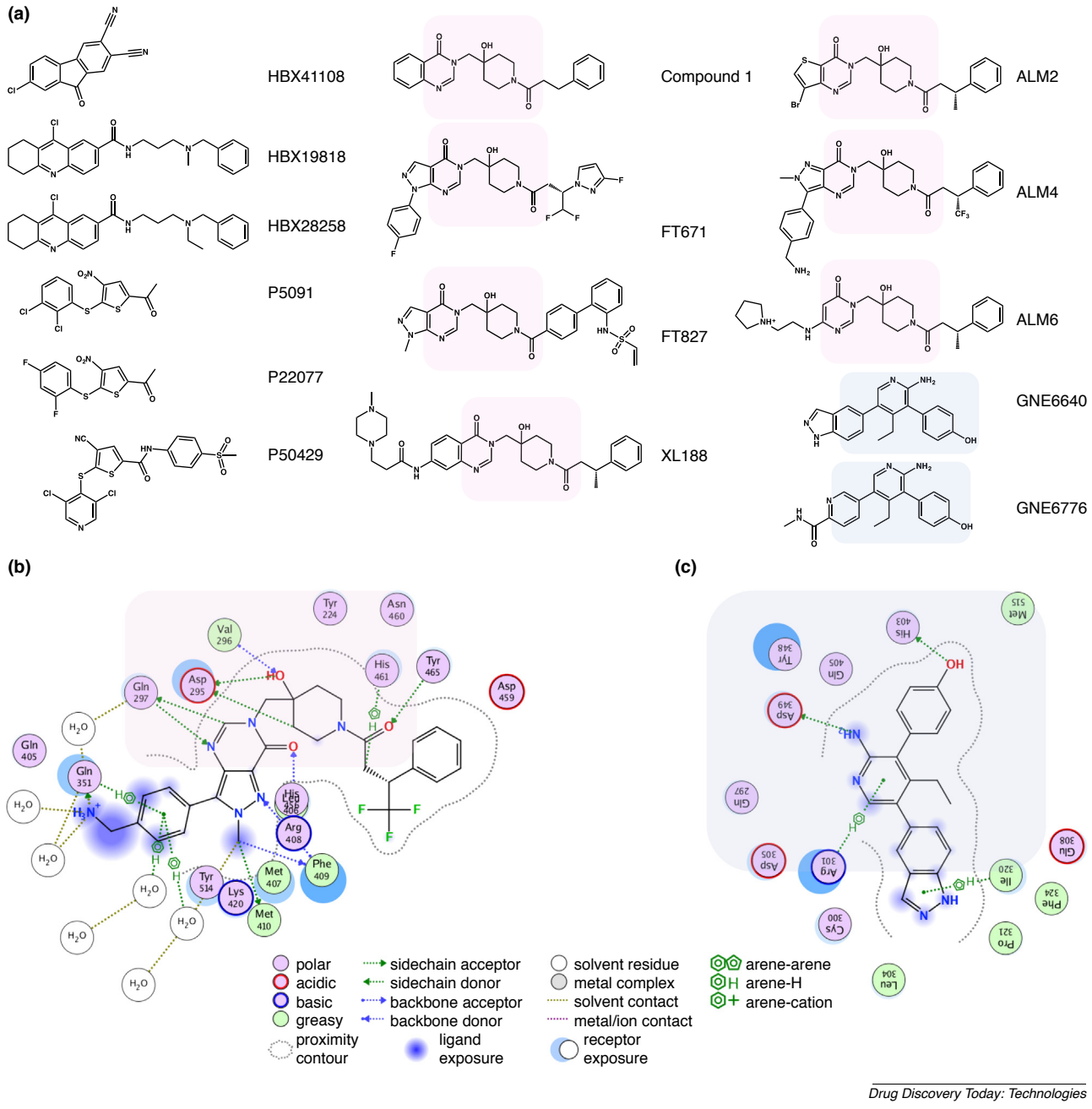

Fig. 3. Chemical structures of small molecule USP7 inhibitors and their representative binding interactions (a) Chemical structures of known USP7 inhibitors (names of the compounds appear to the right of their associated structures). The boxed regions highlight the common chemical sub-structures (continued) continued. (b) 2-D diagram highlighting the common interactions between USP7 and the 4-hydroxypiperidine core (highlighted by the pink box) using PDB-ID 5N9T (c) 2-D diagram highlighting the common interactions between USP7 and non-active site binding compounds (highlighted by the blue box) using PDB-ID 5UQV.

The reversible uncompetitive cyano-indenopyrazine derivative, HBX41108, was initially described as a selective USP7 inhibitor with an IC50 value of 424 nM [65]. However subsequent studies from the same group, suggested HBX41108 was a more potent USP8 inhibitor with an IC50 of 96 nM against USP8 [66]. Similarly, P5091, and other 2-(phenylthio)thiophene-based derivatives such as P22077 and P50429, are dual USP7 and USP47 inhibitors with IC50 values of 4.2/4.3 μM, and 8.2/8.7 μM and 0.42/1.0 μM against USP7/USP47, respectively [67]. The 9-chloro derivatives of amidotetrahydroacridine, HBX19818 and HBX28259 appeared to be more selective for USP7, however, their weak biochemical potency, with IC50 values of 28.1 and 22.6 μM, respectively, covalent mechanism of action, and almost 5-fold greater cellular potency than biochemical potency (HCT116 IC50 ~2 μM), suggested the liabilities in this series [68]. Interestingly, the

same group described a related series of USP7 selective non-covalent inhibitors based on a quinazolin-4-one core and containing a 4-hydroxypiperidine substituent, with a potency range of 25–50 μM [69,70].

Despite the intensive efforts to develop potent and selective small molecule USP7 inhibitors, a structural insight into the binding interactions has hindered the ability to fully understand the potency and selectivity determinants of these inhibitors. However, six recent publications from four different research groups have provided a unique structural insight into potent and selective small molecule inhibitors that sterically block ubiquitin binding by targeting the active site cleft of USP7 [71–74]) and an allosteric site [75,76]. Structural analysis of the active site inhibitors, bound to USP7 catalytic domain, reveals that they all bind to the inactive conformation of USP7 and contain a number of pharmacophoric features that are shared across the different scaffolds (Fig. 3 and Fig. 4). All of the inhibitors contain the 4-hydroxypiperidine substituent, which makes interactions across the active site cleft. The 4-OH group makes two H-bond interactions with the Asp295 sidechain and the backbone amide nitrogen of Val296. In addition, the crystal structures reveal that the acetyl carbonyl makes a H-bond interaction with Y465 sidechain, the common pyrimidinone core engages a donor acceptor interaction with the Gln297 sidechain, and the carbonyl interacts with the backbone amide nitrogen of Phe409. These common interactions are highlighted in Fig. 3b. The USP7 residues that mediate interactions with the 4-hydroxypiperidine containing inhibitors (Asp295, Val296, Gln297, Phe409 and Tyr465) are highly conserved in most USP enzymes [28]. Instead the unique feature of USP7 is the conformation of the switching loop region. The specificity of the 4-hydroxypiperidine containing series of compounds is derived from their ability to interact with and stabilize the unique switching-loop conformation of USP7.

Structural understanding of FT827 and FT671

CRUK/FORMA Therapeutics developed a series of pyrazolo [3,4-d]pyrimidin-4-one-piperidine compounds into potent and selective USP7 inhibitors that work through either covalent interaction with the catalytic Cys223 (FT827, kinact/Ki = 66 M^{-1} s^{-1}), or through a non-covalent mechanism (FT671, IC50 = 52 nM). Both compounds show a high selectivity towards USP7 when screened against a panel of 38 DUBs at 50 μM and incubation of MCF7 breast cancer cells and cell extracts with FT827 and FT671 demonstrates that both compounds show high selectivity towards USP7 in cells [74]. Co-crystal structure analysis of both FT827 (PDB-ID 5NGF) and FT671 (PDB-ID 5NGE) reveals that both compounds bind across the catalytic cleft and stabilize the inactive conformation of USP7. The 4-hydroxypiperidine moiety engages the Asp295 sidechain and the backbone –NH of Val296. The N7 and the acidic proton at C6 of the pyrimidinone moiety are involved with H-bond interactions with Gln297 sidechain and the C=O of the pyrimidinone makes a H-bond with the backbone –NH of Phe409. The pyrazole of the pyrazolo[3,4-

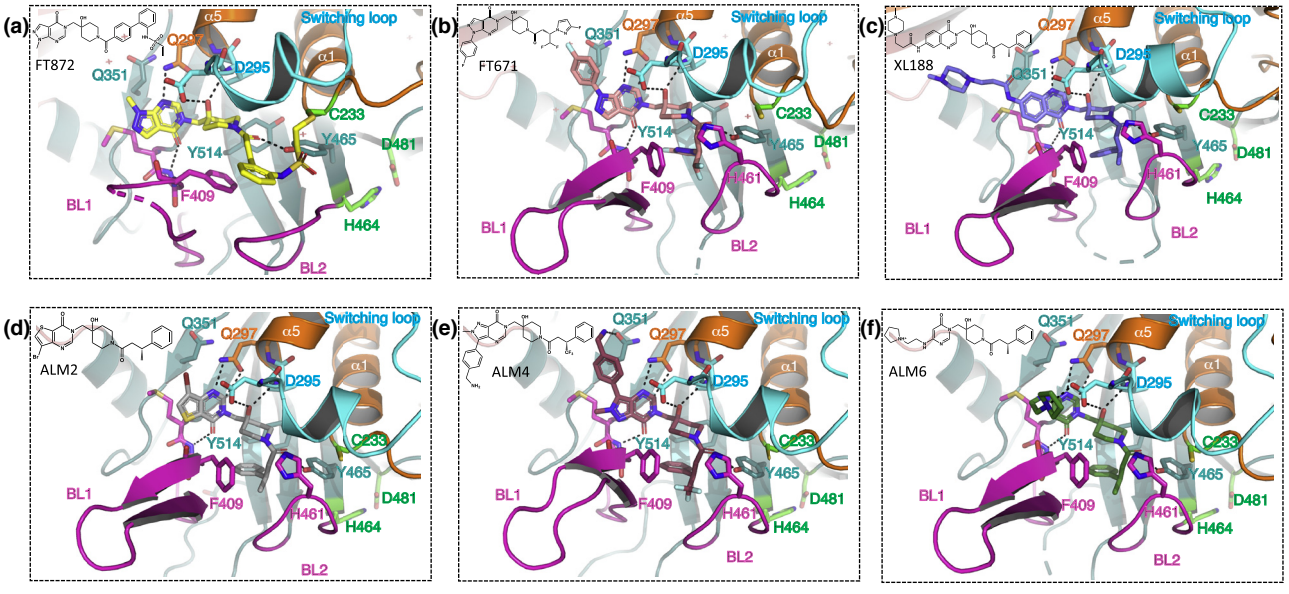

Fig. 4. Crystal structures of USP7 catalytic domain in complex with small molecule inhibitors that target the substrate binding cleft. All inhibitors stabilize the inactive conformation of USP7 and block the access of ubiquitin C-terminal to the catalytic Cys233. (a) USP7 in complex with FT827 (PDB-ID 5NGF) (b) USP7 in complex with FT671 (PDB-ID 5NGE) (c) USP7 in complex with XL188 (PDB-ID 5VS6) (d) USP7 in complex with ALM2 (PDB-ID 5N9R) (e) USP7 in complex with ALM4 (PDB-ID 5N9T) (f) USP7 in complex with ALM6 (PDB-ID 6F5H).

d]pyrimidin-4-one ring system lays on top of the Met407 sidechain and the different substituents at the N1 position directed towards the Gln351 sidechain but do not make a direct interaction. The para-fluorophenyl of FT671 extends over the palm sub-domain and is in van der Waals distance of the methylene atoms of the Gln351 sidechain. Another key feature that both structures reveal is the H-bond interaction between the C=O of the acetyl and the Y465 sidechain.

FT827 and FT671 have different binding interactions with BL1, BL2, the switching loop, and the catalytic Cys223. FT827 stabilizes BL1 and BL2 in similar conformations as those observed in the apo structure of inactive USP7. However, the biphenyl of FT827 pushes up against the switching loop resulting in a slight change in its conformation with the Met292 sidechain from the switching loop lying on top of the terminal phenyl ring. These interactions, together with the interactions between BL2 and the sulfonamide, likely influence the trajectory of the vinylsulfone, facilitating the covalent interaction with the catalytic Cys223 (Fig. 4a). In contrast, the non-covalent analog, FT671, stabilizes significantly different conformations of BL1 and BL2 with the Phe409 sidechain moving over 5 Å to allow the 3-fluoropyrazole to hook back into the hydrophobic Phe409 pocket that is created by the conformational change of Phe409. BL2 adopts a conformation that encircles the difluoromethyl with the His461 sidechain from BL2 stacking onto the alkyl linker (Fig. 4b).

Structural understanding of ALM2, ALM4, and ALM6

Fragment-based screening methods coupled with scaffold hopping using published USP7 inhibitors were used to identify the starting points for the development of the potent and selective USP7 inhibitors ALM2, ALM3 and ALM4 with IC50 = 0.3 μM, 0.022 μM and 0.09 μM, respectively, with high selectivity against a panel of 38 DUBs at 100 μM [71,72]. Scaffold morphing of the thieno[3,2-d]pyrimidin-4(3H)-one fragment hit with Compound **1** confirmed that the bicyclic pyrimidinone core can be replaced with furano, pyrazolo, and thiazolo-pyrimidinone analogues without loss in binding potency. Combining substitutions at the C-7 and a chiral methyl group (R stereochemistry) at the benzylic position of the phenethylamide chain led to the identification of ALM2 (for simplicity the compounds reported from Almac Discovery have been prefixed with ALM and numbered according to the order of publication and the crystal structures and do not relate to the numbers in their respective publications). The co-crystal structure of USP7 catalytic domain in complex with ALM2 (PDB-ID 5N9R reveals that the binding interactions of ALM2 are very similar to both FT671 and XL188 with the 4-hydroxypiperidine moiety interacting with the Asp295 sidechain and the backbone –NH of Val296. The N1 and the acidic proton at C2 of the pyrimidinone moiety are involved with H-bond interactions with Gln297 sidechain and the C=O of the pyrimidinone makes a H-bond with the backbone –NH of Phe409. The 7-Br points towards Gln351, with the SAR and structural analysis suggesting a wide range of substituents can be tolerated in this region (Fig. 4d). Scaffold hopping from the thienopyrimidinone to the N-methyl pyrazolopyrimidinone core led to improvements in physicochemical properties. Substitution at the C-3 position with phenylmethanamine led a 50-fold potency gain. The co-crystal structure of ALM4 (PDB-ID 5N9T) reveals that the phenyl ring lies on top the Gln351 sidechain while the methylamine engages Gln351 sidechain in a H-bond interaction (Fig. 4e).

Further scaffold hopping demonstrated that monocyclic pyrimidinones are also tolerated with substitution at the C-6 position of the pyrimidinone ring improving the potency, leading to the identification of ALM6. The co-crystal structure of USP7 catalytic domain in complex with ALM6 (PDB-ID 6F5H) reveals a similar binding mode to ALM2 and ALM4, with the N-4 of the pyrimidinone ring engaging the Gln297 and the C=O forming a H-bond interaction with the backbone –NH of Phe409. The potency gain from the C-6 substituent in this series is explained by the bidentate H-bond interaction between Asp295 and the protonated nitrogen of the pyrrolidine side-chain of ALM6 [71] (Fig. 4f).

Structural understanding of XL188

The patent literature was the starting point for the structure-guided design of the potent and highly selective non-covalent USP7 inhibitor XL188 [69,73]. XL188 has IC50 = 90 nM against full-length USP7 and at 10 μM is highly selective against a panel of 40 diverse DUBs. The co-crystal structure of USP7 catalytic domain in complex with XL188 (PDB-ID 5VS6) reveals that the core recapitulates the binding interactions of the pyrazolo[3,4-d]pyrimidin-4-one-piperidine series, and similar to the 3-fluoropyrazole of FT671, the terminal phenyl of XL188 is accommodated in the Phe409 hydrophobic pocket due to the large conformational change of the Phe409 sidechain and the change in conformation of BL2 (Fig. 4c). The structure-guided approach used in the development of XL188 provides an insight into the potency gain from the additional modifications to the 3-((4-hydroxy-1-(3-phenylpropanoyl)piperidin-4-yl)methyl)quinazolin-4(3H)-one starting point. The co-crystal structure of USP7 catalytic domain in complex with XL1 (7-chloro-3-((4-hydroxy-1-(3-phenylpropanoyl)piperidin-4-yl)methyl)quinazolin-4(3*H*)-one (PDB-ID 5VSB) reveals that XL1 and XL188 have the same binding mode and make very similar interactions with the inactive conformation of USP7. The 100-fold potency gain observed in the development from XL1 to XL188 can be attributed to methyl group of XL188 present at the benzylic position of the phenethylamide chain that stabilizes the bioactive ''hook-like'' conformation and makes multiple intra- and intermolecular van der Waals interactions

and the edge to face pi-pi interactions with Phe409. In addition, the *N*-methyl-3-(4-methylpiperazin-1-yl)propenamide moiety of XL188 lies on top of the Met407 sidechain with the methylpiperazine sidechain extending out across the palm sub-domain and is solvent exposed. The crystal structure of XL8 (PDB-ID 5VSK) shows a flipped binding mode and the interactions are not consistent with other compounds in this series.

Structural understanding of non-active site USP7 inhibitors

Fragment-based screening methods, coupled with scaffold hopping, were used to identify the starting points for the development of the potent USP7 inhibitors, GNE6776 and GNE6640 with IC50 = 1.34 μM and 0.75 μM against full-length USP7 respectively, and high selectivity against a panel of 36 DUBs at 100 μM [75,76]. The crystal structures of USP7 in complex with GNE-6776 and GNE-6640 (PDB-ID 5UQX and 5UQV respectively) demonstrate that both compounds bind to a novel allosteric pocket that is at the interface of the thumb, fingers and palm subdomains and sterically block ubiquitin binding (Fig. 5a). Structural analysis suggests that this allosteric pocket only exists in the inactive conformation of USP7, due to the cleft created by the movement of residues on the α5, α6 helices and β6 sheet. The structures reveal that the phenol moiety of both compounds bind into the hydrophobic cleft with the hydroxy making H-bond interactions with His403 and Gln405. The central aminopyridine ring sits orthogonal to the plane of the phenol with the 4-ethyl directed towards the interior of the cleft, making van der Waals interactions with Leu304 and Phe324, while the 6-amino group is directed towards solvent and picks up a weak H-bond interaction with Asp349. The sidechain of Arg301 lies over the top of the central aminopyridine ring making pi-cation interactions. The amide nitrogen of GNE6776 engages the Asp305 sidechain in a H-bond interaction while the indazole nitrogen of GNE6640 is 4.2 Å away from the sidechain atoms of this residue. However, the indazole of GNE-6640 is involved in extensive edge to face interactions with the Phe324 sidechain while the edge-face interactions between the pyridine of GNE-6776 and the Phe324 sidechain are more restrictive (Fig. 5b & c).

Cellular studies with USP7 inhibitors

Studies with USP7 inhibitors have primarily focused on their efficacy in promoting tumor growth inhibition. In cellular studies, FT671 regulated the MDM2/p53 axis as well as other USP7 substrates including N-Myc, UHRF1, and DNMT1. Additionally, FT671 increased p53 protein levels and promoted tumor growth inhibition of the MM.1S multiple myeloma xenograft model [74]. XL188 also modulated the MDM2/p53 axis in cellular studies and ALM-34 (also described as Compound-4) promoted MDM2 ubiquitination, stabilized p53, and promoted tumor cell death *in vitro* [71–73]. Similarly, GNE-6640 and GNE-6776 modulated the MDM2/p53 axis and promoted USP7-dependent death in cellular studies. Interestingly cell death was not p53-dependent in a panel of 441 cell lines, pointing to additional USP7-regulated pathways in cells. In the EOL-1 xenograft model, GNE-6776 promoted modest tumor growth inhibition, increased p53 and p21 protein levels, and activated caspases [75,76].

USP14 biology

USP14 in oncology

Human USP14, the yeast Ubp6 ortholog, is a proteasome-associated DUB. USP14 activity is enhanced upon proteasome binding, that in turn suppresses global proteasome function via multiple allosteric mechanisms that will be discussed in greater detail below [77–79]. The mechanisms by which USP14 contributes to tumorigenesis are still being elucidated, with most studies focused on evaluating USP14 expression profiles in tumor tissues. More specifically, USP14 overexpression was confirmed by immunohistochemical analysis in lung, breast, and pancreatic adenocarcinomas relative to matched normal tissues. Mechanistically, USP14 knockdown

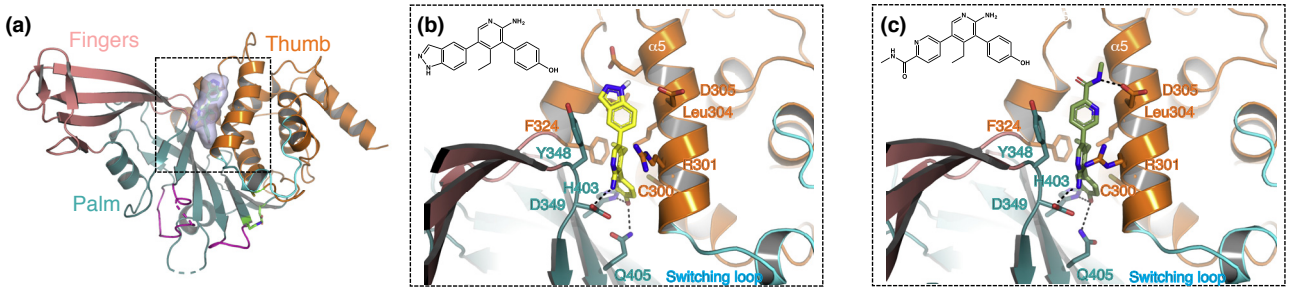

Fig. 5. Crystal structures of USP7 catalytic domain in complex with small molecule inhibitors that bind to an allosteric site in the palm region. All inhibitors stabilize the inactive conformation of USP7 and sterically block ubiquitin binding. (a) The allosteric binding site in the palm region of USP7 with the small molecule inhibitor shown as a surface representation (b) Close in view of GNE-6640 binding (PDB-ID 5UQV) (c) Close in view of GNE-6776 binding (PDB-ID 5UQV).

in cell lines expressing high endogenous USP14 levels slowed *in vitro* proliferation and promoted tumor growth inhibition in xenograft studies, whereas exogenous USP14 expression in cell lines having low endogenous USP14 levels accelerated proliferation [80]. Overexpression of USP14 was also reported in esophageal squamous cell carcinoma, that was significantly associated with distant metastasis and was related to poorer overall patient survival [81]. In gastric cancer, elevated USP14 expression was also an independent prognostic factor for patient survival. Interestingly USP14 knockdown inactivated Akt and ERK signaling pathways and triggered cisplatin-induced apoptosis [82]. The link between USP14 and AKT may therefore be multifaceted, because AKT-induced phosphorylation activates USP14 and thereby attenuates degradation of short-lived proteins, that may in turn promote tumor cell proliferation [83]. The collective data thus point to USP14 as a potential target in a variety of cancers.

USP14 in neurology

As mentioned above, USP14 regulates proteasome activity and is therefore critical for general protein homeostasis. *Ataxia* (ax^J) mice harbor an insertion in the *Usp14* gene to result in nearly complete loss of USP14 expression and provide a useful experimental model of USP14 function. *Ataxia* mice have resting tremors, hind-limb paralysis, and die perinatally due to synaptic transmission defects in their central and peripheral nervous systems [84]. Rescue of the *ataxia* mutants with neuronal-targeted expression of *Usp14* restored viability and motor system function [85]. Additional studies revealed reduced numbers of vesicles in synapses from *ataxia* mice, that likely contribute to compromised synaptic transmission. Interestingly, over-expression of catalytically inactive USP14 in *ataxia* mice restores synaptic vesicle number and corrects hippocampal synaptic transmission deficits [86,87], and transgenic expression of catalytically inactive USP14 in the nervous system of wild-type mice corrected the decreased lifespan that was also observed in *ataxia* mice but not the neuromuscular deficits [88]. Thus, USP14 noncatalytic functions are also important for maintaining normal physiology. This function appears to be conserved since Ubp6, the yeast ortholog of USP14, also regulates conformational dynamics and substrate degradation of the yeast proteasome [89]. Intriguingly, monomeric ubiquitin levels are reduced in *ataxia* mice [90]. Transgenic complementation with neuronally-expressed ubiquitin prevents the perinatal lethality and corrects neuromuscular deficits of *ataxia* mice, indicating that dysregulation of ubiquitin homeostasis due to decreased USP14 expression also contributes to pathogenesis [91].

USP14 is also reported to regulate autophagy, another major system for intracellular protein degradation. This association was first reported in 2016 when Xu and colleagues found that Akt-mediated phosphorylation of USP14 also negatively regulates autophagy. Mass spectrometry studies revealed that USP14 removes K63-linked ubiquitin chains from Beclin-1, a positive regulator of autophagy. More specifically, inhibition of Akt or USP14 function enhanced K63-modified Beclin-1 and autophagic flux in H4 neuroglioma and HEK293 cell lines [92]. These findings were corroborated by Kim and colleagues, who showed that protein degradation is accelerated in USP14 null murine embryonic fibroblasts (MEFs) via both proteasome- and autophagy-regulated pathways [79]. Interestingly another study confirmed that knockdown or deletion of USP14 enhanced cellular proteasome activity, but impaired autophagy flux at the autophagosome/lysosome fusion step. Thus, the role of USP14 in regulating autophagy merits additional study [93]. Chakraborty and colleagues recently reported that USP14 knockdown enhances mitochondrial autophagy (mitophagy) and corrects a *Drosophila* model of Parkinson's disease [94]. Given the potential therapeutic applications, USP14 inhibitors have been developed with the goal of accelerating cellular protein degradation for oncology, neurodegeneration, and other indications such as infectious disease [95].

Mechanisms of USP14 inhibitors

USP14 structural biology

Ubiquitin-specific protease-14 (USP14) is a DUB that reversibly associates with 19S regulatory particle of the proteasome [96]. Full-length human USP14 consists of two structural domains: a 9-kDa N-terminal ubiquitin-like (UBL) domain (residues 1-80) and a 45-kDa C-terminal DUB domain (residues 96-494) [97]. When associated with the proteasome, USP14 removes ubiquitin chains from the proteasome bound substrates, which negatively regulates the activity of the proteasome [77,78,96,98]. USP14 has a high affinity for the proteasome, determined to be around 4 nM [77]. Interestingly, in the proteasome-free state, the catalytic domain of USP14 exhibits a low level of deubiquitinase activity, but when bound to the proteasome, the Ub–AMC hydrolysing activity of USP14 is increased 800-fold over that of isolated USP14 and shows a preference for substrates that are ubiquitinated at more than one site [77,78].

The catalytic domain of USP14 has the same architecture as USP7, resembling an extended hand with Fingers, Thumb and Palm subdomains [57,97] (Fig. 6a). The Fingers subdomain comprise five β-strands (β2–β4, β6, and β7), the Thumb subdomain contains 6 α-helices (α1–α6) and one short β-strand (β1), and the Palm subdomain consists of a six-stranded β-sheet (β5, β8, β10–β13), three α-helices (α7–α9), one short β-strand (β9), and several surface loops. In contrast to the crystal structure of USP7 catalytic domain, the residues that form the catalytic triad of USP14 (Cys114, His435, and Asp451) are aligned in a catalytically competent conformation. However, similar to USP7, the two surface loops close to the active site, blocking loops 1 and 2 (BL1,

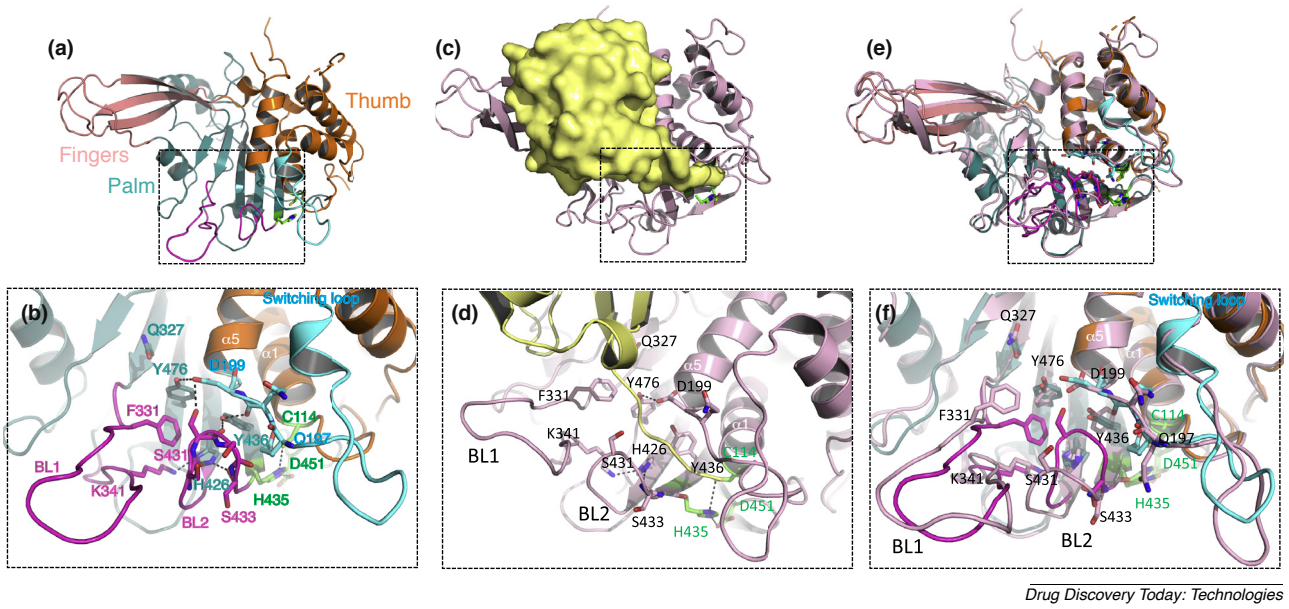

Fig. 6. Crystal structures of USP14 catalytic domain in the inactive (PDB-ID 2AYN) and active conformation with ubiquitin aldehyde (PDB-ID 2AYO). (a) The Fingers, Palm and Thumb sub-domains of inactive USP14 are colored pink, blue and orange respectively. (b) The active site cleft of inactive USP14 with important residues labeled and the catalytic triad colored green. (c) Crystal structure of USP14 catalytic domain in complex with ubiquitin aldehyde. Ubiquitin aldehyde is shown in a surface representation and colored yellow. (d) Active site cleft of USP14 in complex with ubiquitin with important residues labeled and the catalytic triad colored green. (e) Superposition of the inactive and active forms reveals the large conformational changes that occur in α5, the switching loop, BL1, BL2, and the catalytic triad. (f) Comparison of the active site cleft of USP7 in the inactive conformation and in complex with ubiquitin.

resides 254-279 and BL2, residues 429–433), partially occlude the active site cleft that binds the C-terminus of ubiquitin (Fig. 6b). These two surface loops are thought to be responsible for the auto-inhibited state of USP14 in the proteasome-free form since the sidechain of Phe331 on BL1 and the H-bond interaction between Ser431 sidechain on BL2 and Asp199 on the switching loop sterically occlude the substrate binding cleft (Fig. 6b). Comparison of the structures of USP14 catalytic domain and the USP14-Ubiquitin complex reveal that BL1 and BL2 undergo significant conformational changes to accommodate the C-terminal tail of ubiquitin, with only small changes in the conformation of the switching loop [97] (Fig. 6d & f). The activity of USP14 has also been shown to be regulated by post-translational modification of Ser432, which is located within BL2, when this residue is phosphorylated USP14 activity is significantly increased [83].

USP14 inhibitor structural biology

Due to the low level of catalytic activity of free USP14, researchers developed an elegant procedure for isolating USP14 free proteasomes in which the endogenous DUB activity is irreversibly inhibited by ubiquitin vinylsulfone (Ub-VS) and then reconstituting the DUB activity of VS-proteasomes with recombinant USP14. A high throughput screen of 63,052 compounds against recombinant USP14 bound to the VS-proteasome using Ub-AMC as the assay substrate led to the identification IU1, with an IC50 = 4–5 μM against USP14, and good selectivity against a panel of 8 human DUBs [77] (Fig. 7a). The chemical structure of IU1 suggested a covalent mechanism of inhibition, subsequent optimization of IU1 using traditional medicinal chemistry techniques led to the identification of IU1-47, with an IC50 = 0.6 μM against USP14 and good selectivity over IsoT/USP5 [99]. As in the case of USP7, a structural insight into the binding interactions has hindered the ability to develop more potent and selective USP14 inhibitors. However, recent crystal structures of USP14 catalytic domain in complex with IU1, IU1-47, IU1-206, IU1-248 reveal that compounds in this series bind across the catalytic cleft of USP14 and inhibit USP14 activity by non-covalently blocking access of the C-terminal tail of ubiquitin to the active site residues [100] (Fig. 7b–d).

Other small molecule inhibitors of USP14 have been identified from a cell-based screen conducted to identify modulators of the lysosomal apoptosis pathway [101]. The chalcone-based dual USP14/UCHL5 inhibitor, named b-AP15, is thought to inhibit by a covalent mechanism. Although this compound series was ultimately developed into a clinical candidate VLX1570 [102], the mechanism and binding mode of these inhibitors is unknown and therefore will not be discussed further.

Structural understanding of IU1, IU1-47, IU1-206 and IU1-248

The crystal structures of USP14 catalytic domain in complex with that IU1 (PDB-ID 6IIK), IU1-47 (PDB-ID 6IIL), IU1-206 (PDB-ID 6IIM), and IU1-248 (PDB-ID 6IIN) reveal that all

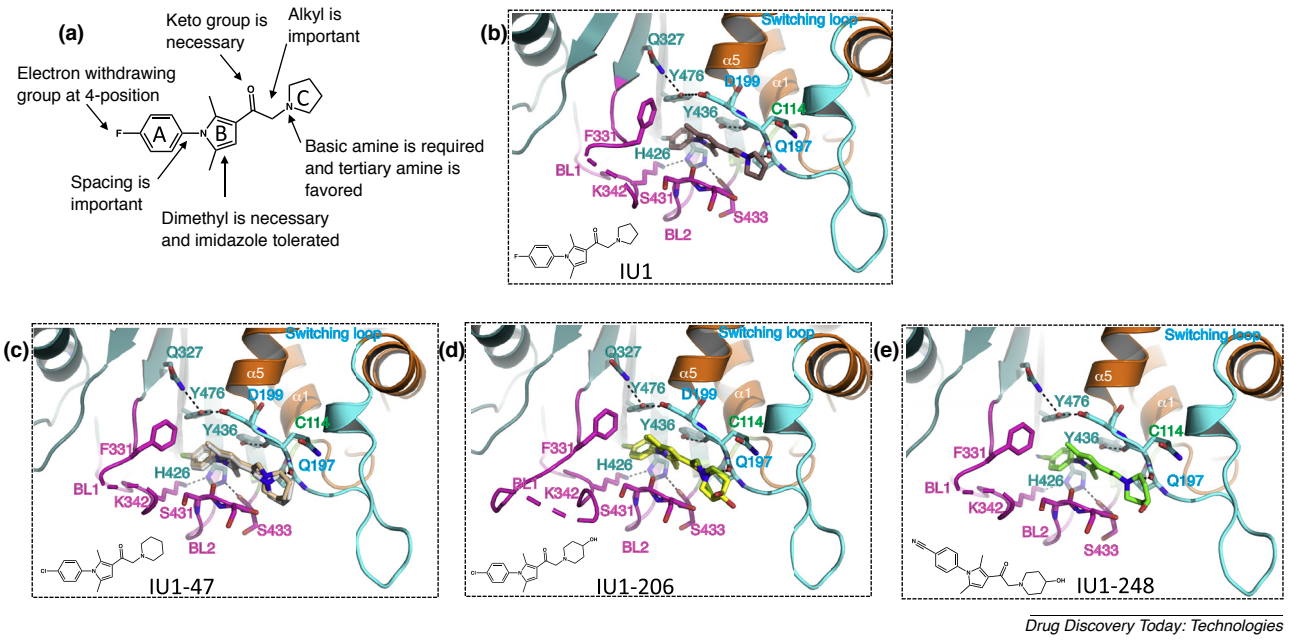

Fig. 7. SAR and structures of IU1 based inhibitors of USP14. (a) SAR trends of IU1 analogs, adapted from Boselli et al. [99] (b) Crystal structure of USP14 catalytic domain in complex with IU1 (PDB-ID 6IIK) (c) Crystal structure of USP14 catalytic domain in complex with IU1-47 (PDB-ID 6IIL) (d) Crystal structure of USP14 catalytic domain in complex with IU1-206 (PDB-ID 6IIM) (e) Crystal structure of USP14 catalytic domain in complex with IU1-248 (PDB-ID 6IIN).

these compounds have very similar interactions with USP14 [100] (Fig. 7b–e). The phenyl A ring of IU1 binds into the Phe331 pocket and makes pi-pi stacking interactions with the sidechain of His426 and edge to face interactions with Phe331 and Tyr476. The halogen in the 4-position of IU1, IU1-47 and IU1-206 makes van der Waals interactions with the methylene atoms of K341. The dimethylpyrrole is orthogonal to the plane of the A-ring with the 2-methyl directed into the Phe331 hydrophobic pocket and the 5-methyl pointing up and making van der Waals contacts with the Phe331 sidechain, this Phe331 pocket is equivalent to the Phe409 pocket observed in USP7. The pyrrole is involved in stacking interactions with the Asp199 sidechain on the switching loop. Interestingly, the keto group does not appear to be making any specific interactions with the protein and likely serves to enforce planarity. The tertiary amide is likely involved in a H-bond interaction with the backbone C=O of Gln197 on the switching loop, which explains the importance of the alkyl chain length. The H-bond interaction between the tertiary amide is not observed in all the crystal structures since the conformations of the pyrrolidine (IU1) and piperidine rings (IU1-47, IU1-206 and IU1-248) are different in the different molecules in the asymmetric units. The improved potency of IU1-47 compared to IU1 can be explained by improved interactions of the larger 4-Cl in IU1-47 and improved van der Waals interactions with residues on the switching loop and Ser432 on BL2 as a result of the bulkier piperidine C-ring. In the crystal structure of USP14 in complex with IU1-206 and IU1-248 the hydroxyl group of the 4-hydoxypiperidine is in different conformations in each of the two molecules in the asymmetric units and this group does not make any specific interactions in either. Wang et al. report the activity and the structure of the benzonitrile derivative of IU1-206, with an IC50 = 0.83 μM suggesting that the polar nitrile group makes less favorable interactions compared to the 4-Cl in IU1-47, in the hydrophobic Phe331 pocket [100].

Cellular studies with USP14 inhibitors

The first USP14 inhibitor, IU1, was evaluated in cellular studies in which proteotoxic proteins, such as tau, TDP-43, ATXN3, and glial fibrillary acidic protein (GFAP), were exogenously expressed in MEFs. IU1 enhanced proteotoxic protein turnover, that was attenuated in USP14-null MEFs indicating a USP14-selective effect. IU1 treatment also increased proteasomal clearance of damaged proteins and enhanced the viability of HEK293 cells challenged with oxidizing agents that promote pathogenic protein aggregation [77]. Boselli et al. confirmed that the more potent IU1 derivative IU1-47 promoted endogenous tau degradation in murine primary neurons and in human iPSC-derived neurons [99]. Consistent with these findings, IU1 treatment reduced protein aggregates and enhanced proteasome functionality in a murine cerebral ischemia/reperfusion injury model, that correlated with reduced infarct volume, decreased neuronal loss, and increased survival in IU1-treated mice [103]. Furthermore, VerPlank et al. reported increased levels of proteasome-associated USP14 in a model of hereditary peripheral neuropathy, and that both IU1 and IU1-47 enhanced protein turnover and degradation of unfolded protein response me-

diator proteins in peripheral nerves [104]. IU1 treatment also mimicked USP14 knockdown or knockout in the above-mentioned studies performed by the Goldberg and Lee labs. More specifically, IU1 treatment enhanced turnover of both proteasome- and autophagy-regulated proteins in the Goldberg lab studies [79]. In the Lee lab studies clearance of tau, a proteasome-degraded protein, was enhanced but degradation of HTT-Q97, an autophagy-cleared protein, was impeded by IU1 treatment [93]. IU1 treatment corroborated USP14 knockdown to enhance mitophagy and correct mitochondrial dysfunction and locomotion behavior of a *Drosophila* model of Parkinson's disease, as reported by Chakraborty and colleagues [94]. IU1 and analogs are also reported to enhance degradation of cellular oncoproteins including the androgen receptor (AR) and estrogen receptor (ER) [105,106]. Thus USP14 inhibitors, like USP14 knockdown or knockout studies, enhance turnover of proteasome-directed substrates and may also enhance clearance of autophagy-regulated substrates.

Conclusions/summary

Here we have reviewed the physiological and pathologic functions of the USP7 and USP14 deubiquitinases, the structural characterization of the apo enzymes and their associated inhibitors, and cellular and *in vivo* studies utilizing these inhibitors with a focus on oncology and neurodegenerative diseases. Somatic amplification of either USP7 and USP14 is generally associated with tumorigenesis whereas inactivating germline mutations or haploinsufficiency of either USP7 or USP14 is generally associated with neurodevelopmental disorders. Furthermore, cellular and *in vivo* studies indicate that functional inhibition of USP7 has therapeutic benefit in oncology indications whereas USP14 inhibition may benefit oncology and neurodegenerative disorders. Structural characterization of USP7 and USP14 catalytic domains suggest that in the apo form both DUBs adopt unique autoinhibited conformations. The structures in complex with small molecule inhibitors reveal that the inhibitors bind to and stabilize these inactive conformations. The structural understanding of how these inhibitors achieve their effects has definitively confirmed that it is possible to design potent and selective inhibitors of deubiquitinases. Importantly, both USP7 and USP14 inhibitors have shown therapeutic benefit in neurodegeneration and in oncology *in vivo* models. It is our hope that these promising pre-clinical studies will rapidly translate to benefit patients in need.

References

[1] Hershko A, Ciechanover A. Mechanisms of intracellular protein breakdown. Annu Rev Biochem 1982;51:335–64. http://dx.doi.org/10.1146/annurev.bi.51.070182.002003.

[2] Hershko A, Ciechanover A. The ubiquitin system for protein degradation. Annu Rev Biochem 1992;61:761–807. http://dx.doi.org/10.1146/annurev.bi.61.070192.003553.

[3] Behrends C, Harper JW. Constructing and decoding unconventional ubiquitin chains. Nat Struct Mol Biol 2011;18:520–8. http://dx.doi.org/10.1038/nsmb.2066.

[4] Komander D, Rape M. The ubiquitin code. Annu Rev Biochem 2012;81:203–29. http://dx.doi.org/10.1146/annurev-biochem-060310-170328.

[5] Kulathu Y, Komander D. Atypical ubiquitylation – the unexplored world of polyubiquitin beyond Lys48 and Lys63 linkages. Nat Rev Mol Cell Biol 2012;13:508–23. http://dx.doi.org/10.1038/nrm3394.

[6] Mevissen TET, Komander D. Mechanisms of deubiquitinase specificity and regulation. Annu Rev Biochem 2017;86:159–92. http://dx.doi.org/10.1146/annurev-biochem-061516-044916.

[7] Schulman BA, Harper JW. Ubiquitin-like protein activation by E1 enzymes: the apex for downstream signalling pathways. Nat Rev Mol Cell Biol 2009;10:319–31. http://dx.doi.org/10.1038/nrm2673.

[8] Ye Y, Rape M. Building ubiquitin chains: E2 enzymes at work. Nat Rev Mol Cell Biol 2009;10:755–64. http://dx.doi.org/10.1038/nrm2780.

[9] Buetow L, Huang DT. Structural insights into the catalysis and regulation of E3 ubiquitin ligases. Nat Rev Mol Cell Biol 2016;17:626–42. http://dx.doi.org/10.1038/nrm.2016.91.

[10] Pao K-C, Wood NT, Knebel A, Rafie K, Stanley M, Mabbitt PD, et al. Activity-based E3 ligase profiling uncovers an E3 ligase with esterification activity. Nature 2018;556:381–5. http://dx.doi.org/10.1038/s41586-018-0026-1.

[11] Finley D. Recognition and processing of ubiquitin-protein conjugates by the proteasome. Annu Rev Biochem 2009;78:477–513. http://dx.doi.org/10.1146/annurev.biochem.78.081507.101607.

[12] Hymowitz SG, Wertz IE. A20: from ubiquitin editing to tumour suppression. Nat Rev Cancer 2010;10:332–41. http://dx.doi.org/10.1038/nrc2775.

[13] Dikic I. Proteasomal and autophagic degradation systems. Annu Rev Biochem 2017;86:193–224. http://dx.doi.org/10.1146/annurev-biochem-061516-044908.

[14] Schwartz AL, Ciechanover A. Targeting proteins for destruction by the ubiquitin system: implications for human pathobiology. Annu Rev Pharmacol Toxicol 2009;49:73–96. http://dx.doi.org/10.1146/annurev.pharmtox.051208.165340.

[15] Moon S, Lee B-H. Chemically induced cellular proteolysis: an emerging therapeutic strategy for undruggable targets. Mol Cells 2018;41:933–42. http://dx.doi.org/10.14348/molcells.2018.0372.

[16] Salami J, Crews CM. Waste disposal-An attractive strategy for cancer therapy. Science 2017;355:1163–7. http://dx.doi.org/10.1126/science.aam7340.

[17] Deshaies RJ. Proteotoxic crisis, the ubiquitin-proteasome system, and cancer therapy. BMC Biol 2014;12:94. http://dx.doi.org/10.1186/s12915-014-0094-0.

[18] Deshaies RJ. Fresh target for cancer therapy. Nature 2009;458:709–10. http://dx.doi.org/10.1038/458709a.

[19] Nicholson B, Marblestone JG, Butt TR, Mattern MR. Deubiquitinating enzymes as novel anticancer targets. Future Oncol 2007;3:191–9. http://dx.doi.org/10.2217/14796694.3.2.191.

[20] Edelmann MJ, Nicholson B, Kessler BM. Pharmacological targets in the ubiquitin system offer new ways of treating cancer, neurodegenerative disorders and infectious diseases. Expert Rev Mol Med 2011;13:e35. http://dx.doi.org/10.1017/S1462399411002031.

[21] Bedford L, Lowe J, Dick LR, Mayer RJ, Brownell JE. Ubiquitin-like protein conjugation and the ubiquitin-proteasome system as drug targets. Nat Rev Drug Discov 2011;10:29–46. http://dx.doi.org/10.1038/nrd3321.

[22] Jacq X, Kemp M, Martin NMB, Jackson SP. Deubiquitylating enzymes and DNA damage response pathways. Cell Biochem Biophys 2013;67:25–43. http://dx.doi.org/10.1007/s12013-013-9635-3.

[23] Davis MI, Simeonov A. Ubiquitin-specific proteases as druggable targets. Drug Target Rev 2015;2:60–4.

[24] Farshi P, Deshmukh RR, Nwankwo JO, Arkwright RT, Cvek B, Liu J, et al. Deubiquitinases (DUBs) and DUB inhibitors: a patent review. Expert Opin Ther Pat 2015;25:1191–208. http://dx.doi.org/10.1517/13543776.2015.1056737.

[25] Ndubaku C, Tsui V. Inhibiting the deubiquitinating enzymes (DUBs). J Med Chem 2015;58:1581–95. http://dx.doi.org/10.1021/jm501061a.
[26] Harrigan JA, Jacq X, Martin NM, Jackson SP. Deubiquitylating enzymes and drug discovery: emerging opportunities. Nat Rev Drug Discov 2018;17:57–78. http://dx.doi.org/10.1038/nrd.2017.152.
[27] Nijman SMB, Luna-Vargas MPA, Velds A, Brummelkamp TR, Dirac AMG, Sixma TK, et al. A genomic and functional inventory of deubiquitinating enzymes. Cell 2005;123:773–86. http://dx.doi.org/10.1016/j.cell.2005.11.007.
[28] Ye Y, Scheel H, Hofmann K, Komander D. Dissection of USP catalytic domains reveals five common insertion points. Mol Biosyst 2009;5:1797–808. http://dx.doi.org/10.1039/b907669g.
[29] Komander D, Clague MJ, Urbé S. Breaking the chains: structure and function of the deubiquitinases. Nat Rev Mol Cell Biol 2009;10:550–63. http://dx.doi.org/10.1038/nrm2731.
[30] Reyes-Turcu FE, Ventii KH, Wilkinson KD. Regulation and cellular roles of ubiquitin-specific deubiquitinating enzymes. Annu Rev Biochem 2009;78:363–97. http://dx.doi.org/10.1146/annurev.biochem.78.082307.091526.
[31] Worden EJ, Padovani C, Martin A. Structure of the Rpn11-Rpn8 dimer reveals mechanisms of substrate deubiquitination during proteasomal degradation. Nat Struct Mol Biol 2014;21:220–7. http://dx.doi.org/10.1038/nsmb.2771.
[32] Abdul Rehman SA, Kristariyanto YA, Choi S-Y, Nkosi PJ, Weidlich S, Labib K, et al. MINDY-1 is a member of an evolutionarily conserved and structurally distinct new family of deubiquitinating enzymes. Mol Cell 2016;63:146–55. http://dx.doi.org/10.1016/j.molcel.2016.05.009.
[33] Coleman KE, Huang TT. In a class of its own: a new family of deubiquitinases promotes genome stability. Mol Cell 2018;70:1–3. http://dx.doi.org/10.1016/j.molcel.2018.03.022.
[34] Dang LC, Melandri FD, Stein RL. Kinetic and mechanistic studies on the hydrolysis of ubiquitin C-terminal 7-amido-4-methylcoumarin by deubiquitinating enzymes. Biochemistry 1998;37:1868–79. http://dx.doi.org/10.1021/bi9723360.
[35] Hassiepen U, Eidhoff U, Meder G, Bulber J-F, Hein A, Bodendorf U, et al. A sensitive fluorescence intensity assay for deubiquitinating proteases using ubiquitin-rhodamine110-glycine as substrate. Anal Biochem 2007;371:201–7. http://dx.doi.org/10.1016/j.ab.2007.07.034.
[36] El Oualid F, Merkx R, Ekkebus R, Hameed DS, Smit JJ, de Jong A, et al. Chemical synthesis of ubiquitin, ubiquitin-based probes, and diubiquitin. Angew Chem Int Ed Engl 2010;49:10149–53. http://dx.doi.org/10.1002/anie.201005995.
[37] Hewings DS, Flygare JA, Bogyo M, Wertz IE. Activity-based probes for the ubiquitin conjugation-deconjugation machinery: new chemistries, new tools, and new insights. FEBS J 2017;284:1555–76. http://dx.doi.org/10.1111/febs.14039.
[38] Ritorto MS, Ewan R, Perez-Oliva AB, Knebel A, Buhrlage SJ, Wightman M, et al. Screening of DUB activity and specificity by MALDI-TOF mass spectrometry. Nat Commun 2014;5:4763. http://dx.doi.org/10.1038/ncomms5763.
[39] Kramer HB, Nicholson B, Kessler BM, Altun M. Detection of ubiquitin-proteasome enzymatic activities in cells: application of activity-based probes to inhibitor development. Biochim Biophys Acta 2012;1823:2029–37. http://dx.doi.org/10.1016/j.bbamcr.2012.05.014.
[40] Lee JT, Gu W. The multiple levels of regulation by p53 ubiquitination. Cell Death Differ 2010;17:86–92. http://dx.doi.org/10.1038/cdd.2009.77.
41]. Cummins JM, Rago C, Kohli M, Kinzler KW, Lengauer C, Vogelstein B. Tumour suppression: disruption of HAUSP gene stabilizes p53. Nature 2004;428. http://dx.doi.org/10.1038/nature02501. 1 p following 486.
[42] Kon N, Kobayashi Y, Li M, Brooks CL, Ludwig T, Gu W. Inactivation of HAUSP in vivo modulates p53 function. Oncogene 2010;29:1270–9. http://dx.doi.org/10.1038/onc.2009.427.
[43] Kon N, Zhong J, Kobayashi Y, Li M, Szabolcs M, Ludwig T, et al. Roles of HAUSP-mediated p53 regulation in central nervous system development. Cell Death Differ 2011;18:1366–75. http://dx.doi.org/10.1038/cdd.2011.12.
[44] Meulmeester E, Maurice MM, Boutell C, Teunisse AFAS, Ovaa H, Abraham TE, et al. Loss of HAUSP-mediated deubiquitination contributes to DNA damage-induced destabilization of Hdmx and Hdm2. Mol Cell 2005;18:565–76. http://dx.doi.org/10.1016/j.molcel.2005.04.024.
[45] Marx JL. The N-myc oncogene in neural tumors. Science 1984;224:1088.
[46] Tavana O, Li D, Dai C, Lopez G, Banerjee D, Kon N, et al. HAUSP deubiquitinates and stabilizes N-Myc in neuroblastoma. Nat Med 2016;22:1180–6. http://dx.doi.org/10.1038/nm.4180.
[47] Georges A, Marcon E, Greenblatt J, Frappier L. Identification and characterization of USP7 targets in cancer cells. Sci Rep 2018;8:15833. http://dx.doi.org/10.1038/s41598-018-34197-x.
[48] Zhou J, Wang J, Chen C, Yuan H, Wen X, Sun H. USP7: target validation and drug discovery for cancer therapy. Med Chem 2018;14:3–18. http://dx.doi.org/10.2174/1573406413666171020115539.
[49] Cole AJ, Clifton-Bligh R, Marsh DJ. Histone H2B monoubiquitination: roles to play in human malignancy. Endocr Relat Cancer 2015;22:T19–33. http://dx.doi.org/10.1530/ERC-14-0185.
[50] van der Knaap JA, Kumar BRP, Moshkin YM, Langenberg K, Krijgsveld J, Heck AJR, et al. GMP synthetase stimulates histone H2B deubiquitylation by the epigenetic silencer USP7. Mol Cell 2005;17:695–707. http://dx.doi.org/10.1016/j.molcel.2005.02.013.
[51] Sarkari F, Sanchez-Alcaraz T, Wang S, Holowaty MN, Sheng Y, Frappier L. EBNA1-mediated recruitment of a histone H2B deubiquitylating complex to the Epstein-Barr virus latent origin of DNA replication. PLoS Pathog 2009;5:e1000624. http://dx.doi.org/10.1371/journal.ppat.1000624.
[52] Faesen AC, Dirac AMG, Shanmugham A, Ovaa H, Perrakis A, Sixma TK. Mechanism of USP7/HAUSP activation by its C-terminal ubiquitin-like domain and allosteric regulation by GMP-synthetase. Mol Cell 2011;44:147–59. http://dx.doi.org/10.1016/j.molcel.2011.06.034.
[53] Huether R, Dong L, Chen X, Wu G, Parker M, Wei L, et al. The landscape of somatic mutations in epigenetic regulators across 1,000 paediatric cancer genomes. Nat Commun 2014;5:3630. http://dx.doi.org/10.1038/ncomms4630.
[54] Tacer KF, Potts PR. Cellular and disease functions of the Prader-Willi Syndrome gene MAGEL2. Biochem J 2017;474:2177–90. http://dx.doi.org/10.1042/BCJ20160616.
[55] Hao Y-H, Fountain MD, Fon Tacer K, Xia F, Bi W, Kang S-HL, et al. USP7 acts as a molecular rheostat to promote WASH-dependent endosomal protein recycling and is mutated in a human neurodevelopmental disorder. Mol Cell 2015;59:956–69. http://dx.doi.org/10.1016/j.molcel.2015.07.033.
[56] Kim RQ, Sixma TK. Regulation of USP7: a high incidence of E3 complexes. J Mol Biol 2017;429:3395–408. http://dx.doi.org/10.1016/j.jmb.2017.05.028.
[57] Hu M, Li P, Li M, Li W, Yao T, Wu J-W, et al. Crystal structure of a UBP-family deubiquitinating enzyme in isolation and in complex with ubiquitin aldehyde. Cell 2002;111:1041–54. http://dx.doi.org/10.1016/S0092-8674(02)01199-6.
[58] Saridakis V, Sheng Y, Sarkari F, Holowaty MN, Shire K, Nguyen T, et al. Structure of the p53 binding domain of HAUSP/USP7 bound to Epstein-Barr nuclear antigen 1 implications for EBV-mediated immortalization. Mol Cell 2005;18:25–36. http://dx.doi.org/10.1016/j.molcel.2005.02.029.
[59] Hu M, Gu L, Li M, Jeffrey PD, Gu W, Shi Y. Structural basis of competitive recognition of p53 and MDM2 by HAUSP/USP7: implications for the regulation of the p53-MDM2 pathway. PLoS Biol 2006;4:e27. http://dx.doi.org/10.1371/journal.pbio.0040027.
[60] Cheng J, Yang H, Fang J, Ma L, Gong R, Wang P, et al. Molecular mechanism for USP7-mediated DNMT1 stabilization by acetylation. Nat Commun 2015;6:7023. http://dx.doi.org/10.1038/ncomms8023.
[61] Pfoh R, Lacdao IK, Georges AA, Capar A, Zheng H, Frappier L, et al. Crystal structure of USP7 ubiquitin-like domains with an ICP0 peptide reveals a novel mechanism used by viral and cellular proteins to target USP7. PLoS Pathog 2015;11:e1004950. http://dx.doi.org/10.1371/journal.ppat.1004950.

[62] Rougé L, Bainbridge TW, Kwok M, Tong R, Di Lello P, Wertz IE, et al. Molecular understanding of USP7 substrate recognition and C-terminal activation. Structure 2016;24:1335–45. http://dx.doi.org/10.1016/j.str.2016.05.020.
[63] Molland K, Zhou Q, Mesecar AD. A 2.2 Å resolution structure of the USP7 catalytic domain in a new space group elaborates upon structural rearrangements resulting from ubiquitin binding. Acta Crystallogr Sect F Struct Biol Commun 2014;70:283–7. http://dx.doi.org/10.1107/S2053230X14002519.
[64] Fernández-Montalván A, Bouwmeester T, Joberty G, Mader R, Mahnke M, Pierrat B, et al. Biochemical characterization of USP7 reveals post-translational modification sites and structural requirements for substrate processing and subcellular localization. FEBS J 2007;274:4256–70. http://dx.doi.org/10.1111/j.1742-4658.2007.05952.x.
[65] Colland F, Formstecher E, Jacq X, Reverdy C, Planquette C, Conrath S, et al. Small-molecule inhibitor of USP7/HAUSP ubiquitin protease stabilizes and activates p53 in cells. Mol Cancer Ther 2009;8:2286–95. http://dx.doi.org/10.1158/1535-7163.MCT-09-0097.
[66] Colombo M, Vallese S, Peretto I, Jacq X, Rain J-C, Colland F, et al. Synthesis and biological evaluation of 9-oxo-9H-indeno[1,2-b]pyrazine-2,3-dicarbonitrile analogues as potential inhibitors of deubiquitinating enzymes. ChemMedChem 2010;5:552–8. http://dx.doi.org/10.1002/cmdc.200900409.
[67] Weinstock J, Wu J, Cao P, Kingsbury WD, McDermott JL, Kodrasov MP, et al. Selective dual inhibitors of the cancer-related deubiquitylating proteases USP7 and USP47. ACS Med Chem Lett 2012;3:789–92. http://dx.doi.org/10.1021/ml200276j.
[68] Reverdy C, Conrath S, Lopez R, Planquette C, Atmanene C, Collura V, et al. Discovery of specific inhibitors of human USP7/HAUSP deubiquitinating enzyme. Chem Biol 2012;19:467–77. http://dx.doi.org/10.1016/j.chembiol.2012.02.007.
[69] Colland F, Gourdel ME. 546 Substituted quinazolin-4-ones for inhibiting ubiquitin specific protease 7. US Patent 9. (546).
[70] Kessler BM. Selective and reversible inhibitors of ubiquitin-specific protease 7: a patent evaluation (WO2013030218). Expert Opin Ther Pat 2014;24:597–602. http://dx.doi.org/10.1517/13543776.2014.882320.
[71] O'Dowd CR, Helm MD, Rountree JSS, Flasz JT, Arkoudis E, Miel H, et al. Identification and structure-guided development of pyrimidinone based USP7 inhibitors. ACS Med Chem Lett 2018;9:238–43. http://dx.doi.org/10.1021/acsmedchemlett.7b00512.
[72] Gavory G, O'Dowd CR, Helm MD, Flasz J, Arkoudis E, Dossang A, et al. Discovery and characterization of highly potent and selective allosteric USP7 inhibitors. Nat Chem Biol 2018;14:118–25. http://dx.doi.org/10.1038/nchembio.2528.
[73] Lamberto I, Liu X, Seo H-S, Schauer NJ, Iacob RE, Hu W, et al. Structure-guided development of a potent and selective non-covalent active-site inhibitor of USP7. Cell Chem Biol 2017;24. http://dx.doi.org/10.1016/j.chembiol.2017.09.003. 1490–1500.e11.
[74] Turnbull AP, Ioannidis S, Krajewski WW, Pinto-Fernandez A, Heride C, Martin ACL, et al. Molecular basis of USP7 inhibition by selective small-molecule inhibitors. Nature 2017;550:481–6. http://dx.doi.org/10.1038/nature24451.
[75] Kategaya L, Di Lello P, Rougé L, Pastor R, Clark KR, Drummond J, et al. USP7 small-molecule inhibitors interfere with ubiquitin binding. Nature 2017;550:534–8. http://dx.doi.org/10.1038/nature24006.
[76] Di Lello P, Pastor R, Murray JM, Blake RA, Cohen F, Crawford TD, et al. Discovery of small-molecule inhibitors of ubiquitin specific protease 7 (USP7) using integrated NMR and in silico techniques. J Med Chem 2017;60:10056–70. http://dx.doi.org/10.1021/acs.jmedchem.7b01293.
[77] Lee B-H, Lee MJ, Park S, Oh D-C, Elsasser S, Chen P-C, et al. Enhancement of proteasome activity by a small-molecule inhibitor of USP14. Nature 2010;467:179–84. http://dx.doi.org/10.1038/nature09299.
[78] Lee B-H, Lu Y, Prado MA, Shi Y, Tian G, Sun S, et al. USP14 deubiquitinates proteasome-bound substrates that are ubiquitinated at multiple sites. Nature 2016;532:398–401. http://dx.doi.org/10.1038/nature17433.
[79] Kim HT, Goldberg AL. The deubiquitinating enzyme Usp14 allosterically inhibits multiple proteasomal activities and ubiquitin-independent proteolysis. J Biol Chem 2017;292:9830–9. http://dx.doi.org/10.1074/jbc.M116.763128.
[80] Zhu Y, Zhang C, Gu C, Li Q, Wu N. Function of deubiquitinating enzyme USP14 as oncogene in different types of cancer. Cell Physiol Biochem 2016;38:993–1002. http://dx.doi.org/10.1159/000443051.
[81] Zhang B, Li M, Huang P, Guan X-Y, Zhu Y-H. Overexpression of ubiquitin specific peptidase 14 predicts unfavorable prognosis in esophageal squamous cell carcinoma. Thorac Cancer 2017;8:344–9. http://dx.doi.org/10.1111/1759-7714.12453.
[82] Fu Y, Ma G, Liu G, Li B, Li H, Hao X, et al. USP14 as a novel prognostic marker promotes cisplatin resistance via Akt/ERK signaling pathways in gastric cancer. Cancer Med 2018;7:5577–88. http://dx.doi.org/10.1002/cam4.1770.
[83] Xu D, Shan B, Lee B-H, Zhu K, Zhang T, Sun H, et al. Phosphorylation and activation of ubiquitin-specific protease-14 by Akt regulates the ubiquitin-proteasome system. Elife 2015;4:e10510. http://dx.doi.org/10.7554/eLife.10510.
[84] Wilson SM, Bhattacharyya B, Rachel RA, Coppola V, Tessarollo L, Householder DB, et al. Synaptic defects in ataxia mice result from a mutation in Usp14, encoding a ubiquitin-specific protease. Nat Genet 2002;32:420–5. http://dx.doi.org/10.1038/ng1006.
[85] Crimmins S, Jin Y, Wheeler C, Huffman AK, Chapman C, Dobrunz LE, et al. Transgenic rescue of ataxia mice with neuronal-specific expression of ubiquitin-specific protease 14. J Neurosci 2006;26:11423–31. http://dx.doi.org/10.1523/JNEUROSCI.3600-06.2006.
[86] Bhattacharyya BJ, Wilson SM, Jung H, Miller RJ. Altered neurotransmitter release machinery in mice deficient for the deubiquitinating enzyme Usp14. Am J Physiol Cell Physiol 2012;302:C698–708. http://dx.doi.org/10.1152/ajpcell.00326.2010.
[87] Walters BJ, Hallengren JJ, Theile CS, Ploegh HL, Wilson SM, Dobrunz LE. A catalytic independent function of the deubiquitinating enzyme USP14 regulates hippocampal synaptic short-term plasticity and vesicle number. J Physiol (Lond) 2014;592:571–86. http://dx.doi.org/10.1113/jphysiol.2013.266015.
[88] Vaden JH, Bhattacharyya BJ, Chen P-C, Watson JA, Marshall AG, Phillips SE, et al. Ubiquitin-specific protease 14 regulates c-Jun N-terminal kinase signaling at the neuromuscular junction. Mol Neurodegener 2015;10:3. http://dx.doi.org/10.1186/1750-1326-10-3.
[89] Bashore C, Dambacher CM, Goodall EA, Matyskiela ME, Lander GC, Martin A. Ubp6 deubiquitinase controls conformational dynamics and substrate degradation of the 26S proteasome. Nat Struct Mol Biol 2015;22:712–9. http://dx.doi.org/10.1038/nsmb.3075.
[90] Anderson C, Crimmins S, Wilson JA, Korbel GA, Ploegh HL, Wilson SM. Loss of Usp14 results in reduced levels of ubiquitin in ataxia mice. J Neurochem 2005;95:724–31. http://dx.doi.org/10.1111/j.1471-4159.2005.03409.x.
[91] Chen P-C, Bhattacharyya BJ, Hanna J, Minkel H, Wilson JA, Finley D, et al. Ubiquitin homeostasis is critical for synaptic development and function. J Neurosci 2011;31:17505–13. http://dx.doi.org/10.1523/JNEUROSCI.2922-11.2011.
[92] Xu D, Shan B, Sun H, Xiao J, Zhu K, Xie X, et al. USP14 regulates autophagy by suppressing K63 ubiquitination of Beclin 1. Genes Dev 2016;30:1718–30. http://dx.doi.org/10.1101/gad.285122.116.
[93] Kim E, Park S, Lee JH, Mun JY, Choi WH, Yun Y, et al. Dual function of USP14 deubiquitinase in cellular proteasomal activity and autophagic flux. Cell Rep 2018;24:732–43. http://dx.doi.org/10.1016/j.celrep.2018.06.058.
[94] Chakraborty J, von Stockum S, Marchesan E, Caicci F, Ferrari V, Rakovic A, et al. USP14 inhibition corrects an in vivo model of impaired mitophagy. EMBO Mol Med 2018;10. http://dx.doi.org/10.15252/emmm.201809014.
[95] de Poot SAH, Tian G, Finley D. Meddling with fate: the proteasomal deubiquitinating enzymes. J Mol Biol 2017;429:3525–45. http://dx.doi.org/10.1016/j.jmb.2017.09.015.
[96] Koulich E, Li X, DeMartino GN. Relative structural and functional roles of multiple deubiquitylating proteins associated with mammalian 26S

proteasome. Mol Biol Cell 2008;19:1072–82. http://dx.doi.org/10.1091/mbc.E07-10-1040.

[97] Hu M, Li P, Song L, Jeffrey PD, Chenova TA, Wilkinson KD, et al. Structure and mechanisms of the proteasome-associated deubiquitinating enzyme USP14. EMBO J 2005;24:3747–56. http://dx.doi.org/10.1038/sj.emboj.7600832.

[98] Borodovsky A, Kessler BM, Casagrande R, Overkleeft HS, Wilkinson KD, Ploegh HL. A novel active site-directed probe specific for deubiquitylating enzymes reveals proteasome association of USP14. EMBO J 2001;20:5187–96. http://dx.doi.org/10.1093/emboj/20.18.5187.

[99] Boselli M, Lee B-H, Robert J, Prado MA, Min S-W, Cheng C, et al. An inhibitor of the proteasomal deubiquitinating enzyme USP14 induces tau elimination in cultured neurons. J Biol Chem 2017;292:19209–25. http://dx.doi.org/10.1074/jbc.M117.815126.

[100] Wang Y, Jiang Y, Ding S, Li J, Song N, Ren Y, et al. Small molecule inhibitors reveal allosteric regulation of USP14 via steric blockade. Cell Res 2018;28:1186–94. http://dx.doi.org/10.1038/s41422-018-0091-x.

[101] D'Arcy P, Brnjic S, Olofsson MH, Fryknäs M, Lindsten K, De Cesare M, et al. Inhibition of proteasome deubiquitinating activity as a new cancer therapy. Nat Med 2011;17:1636–40. http://dx.doi.org/10.1038/nm.2536.

[102] Wang X, D'Arcy P, Caulfield TR, Paulus A, Chitta K, Mohanty C, et al. Synthesis and evaluation of derivatives of the proteasome deubiquitinase inhibitor b-AP15. Chem Biol Drug Des 2015;86:1036–48. http://dx.doi.org/10.1111/cbdd.12571.

[103] Min Lü L, Martin DS, Wang H. USP14 inhibitor attenuates cerebral ischemia/reperfusion-induced neuronal injury in mice. J Neurochem 2017;140:826–33. http://dx.doi.org/10.1111/jnc.13941.

[104] VerPlank JJS, Lokireddy S, Feltri ML, Goldberg AL, Wrabetz L. Impairment of protein degradation and proteasome function in hereditary neuropathies. Glia 2018;66:379–95. http://dx.doi.org/10.1002/glia.23251.

[105] Xia X, Liao Y, Guo Z, Li Y, Jiang L, Zhang F, et al. Targeting proteasome-associated deubiquitinases as a novel strategy for the treatment of estrogen receptor-positive breast cancer. Oncogenesis 2018;7:75. http://dx.doi.org/10.1038/s41389-018-0086-y.

[106] Liao Y, Xia X, Liu N, Cai J, Guo Z, Li Y, et al. Growth arrest and apoptosis induction in androgen receptor-positive human breast cancer cells by inhibition of USP14-mediated androgen receptor deubiquitination. Oncogene 2018;37:1896–910. http://dx.doi.org/10.1038/s41388-017-0069-z.